

VISA: Reasoning Video Object Segmentation via Large Language Models

Cilin Yan*
Beihang University

Haochen Wang*
University of Amsterdam

Shilin Yan, Xiaolong Jiang, Yao Hu
Xiaohongshu Inc.

Guoliang Kang†
Beihang University

Weidi Xie
Shanghai Jiao Tong University

Efstathios Gavves
University of Amsterdam

Abstract

Existing Video Object Segmentation (VOS) relies on explicit user instructions, such as categories, masks, or short phrases, restricting their ability to perform complex video segmentation requiring reasoning with world knowledge. In this paper, we introduce a new task, Reasoning Video Object Segmentation (ReasonVOS). This task aims to generate a sequence of segmentation masks in response to implicit text queries that require complex reasoning abilities based on world knowledge and video contexts, which is crucial for structured environment understanding and object-centric interactions, pivotal in the development of embodied AI. To tackle ReasonVOS, we introduce VISA (Video-based large language Instructed Segmentation Assistant), to leverage the world knowledge reasoning capabilities of multi-modal LLMs while possessing the ability to segment and track objects in videos with a mask decoder. Moreover, we establish a comprehensive benchmark consisting of 35,074 instruction-mask sequence pairs from 1,042 diverse videos, which incorporates complex world knowledge reasoning into segmentation tasks for instruction-tuning and evaluation purposes of ReasonVOS models. Experiments conducted on 8 datasets demonstrate the effectiveness of VISA in tackling complex reasoning segmentation and vanilla referring segmentation in both video and image domains. The code and dataset are available at <https://github.com/cilinyan/VISA>.

1. Introduction

Existing video object segmentation relies on explicit queries, such as pre-defined categories [3, 44, 48], masks of certain frames [5, 50], or explicit short phrases describing intuitive features [2, 37, 47]. Such systems lack the capacity to reason and infer users’ intentions based on implicit

instructions. For instance, it is more intuitive for the users to give instructions like “Find my favorite cup” instead of “Find the red cup located second to the left on the table”. To accomplish the first instruction, the model needs to understand that “favorite” means “most frequently used” to some degree, and callback the history temporal information to localize the cup.

In this work, we propose Reasoning Video Object Segmentation (ReasonVOS), which aims to generate a binary mask sequence given complex and implicit text instruction in videos. Notably, the text instruction is not limited to a straightforward reference (e.g., the running car), but a more complex description including reasoning of world knowledge (e.g., the car powered by electricity). This task requires the integration of reasoning ability with long-term video understanding to accurately localize target objects in videos, which is a crucial ability for Embodied AI systems that enable robots to fulfill effective interaction with objects in dynamic environments given user instructions.

To tackle Reasoning Segmentation in images, recent work LISA [17] leverages the language generation prowess of multi-modal LLMs, complemented by a mask decoder for generating segmentation results. However, the Reasoning Segmentation in videos demands temporal information for comprehensive video understanding and spatial details for producing high-quality segmentation mask sequences. Therefore, the multi-modal LLMs need to simultaneously process multiple frames with a substantial number of tokens for each frame. Considering the numerous visual tokens to be processed simultaneously, it is computationally intractable to directly broadcast an image reasoning segmentation model to the video domain.

To this end, we introduce VISA (Video-based large language Instructed Segmentation Assistant), designed to efficiently encode long-term video features while preserving spatial details to enable reasoning in video object segmentation. Specifically, we start by designing a Text-guided Frame Sampler (TFS) to select frames that are most rele-

*Equal contribution.

†Corresponding author.

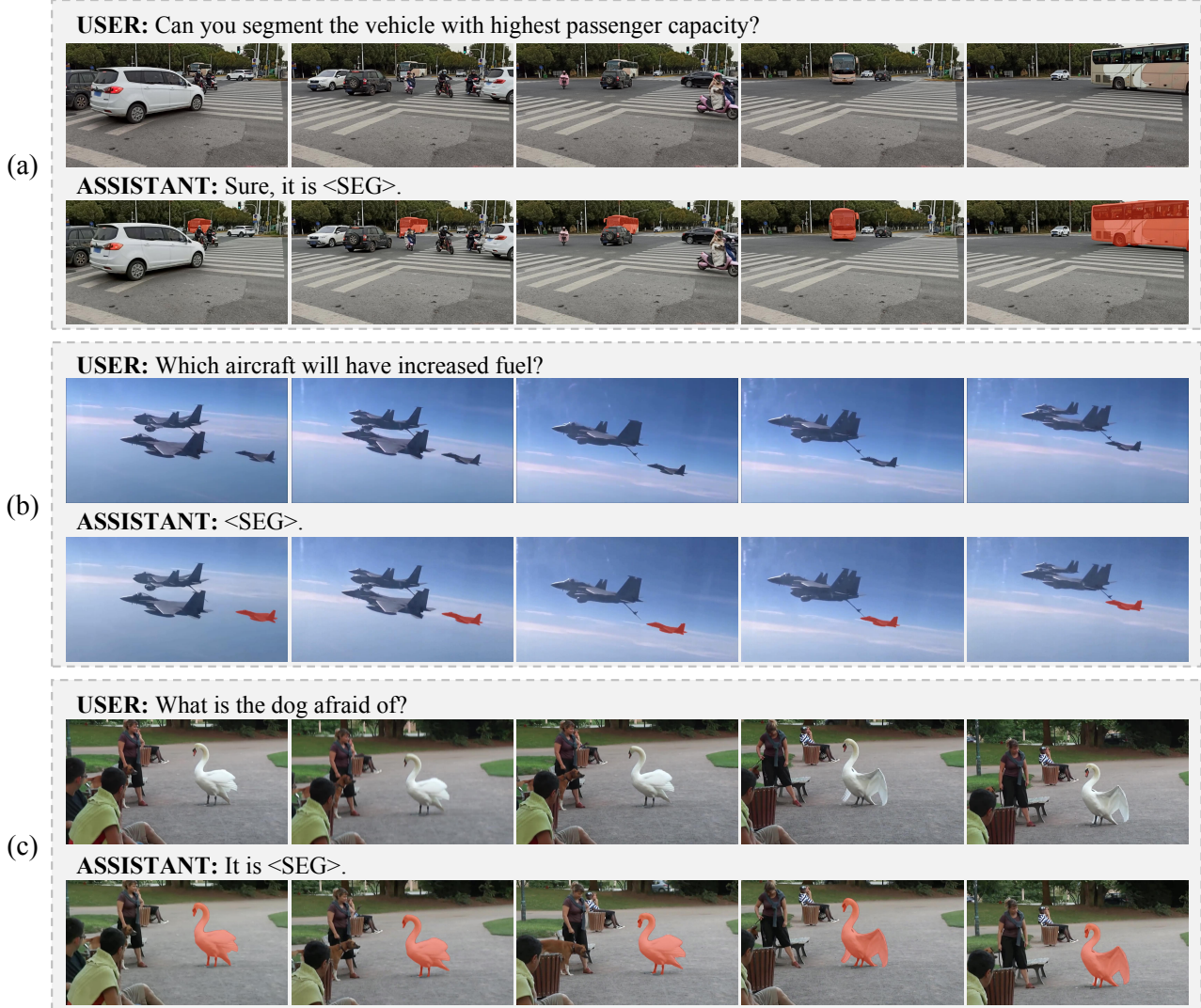


Figure 1. We enable the reasoning video object segmentation capabilities for current multi-modal LLMs. The proposed VISA is capable of segmenting and tracking objects given text descriptions involving: (a) complex reasoning of world knowledge; (b) inference of upcoming events; and (c) comprehensive understanding of video content.

vant to the task based on textual instructions, focusing the model on the most significant moments for object identification. TFS reduces the requirement of visual token numbers to be handled, enabling VISA to process long-term videos. These selected frames, along with the text queries, are tokenized and processed concurrently by a multi-modal Large Language Model (LLM), enabling sophisticated reasoning over video content and facilitating the generation of precise textual outputs. To equip VISA with robust segmentation capabilities, we incorporate a special token `<SEG>` in the output text, inspired by the approach in LISA [17]. The hidden embedding of `<SEG>` is leveraged to produce segmentation masks of selected frames using a SAM [16] decoder. The segmentation process is completed by de-

riving the masks for the remaining frames with an object tracker [4]. As illustrated in Fig. 1, VISA demonstrates remarkable proficiency in handling complex segmentation tasks that require: (a) reasoning based on world knowledge; (b) inference of future events; and (c) a comprehensive understanding of video content.

To evaluate the effectiveness of the proposed VISA, we create a benchmark dataset named ReVOS. This dataset comprises 35,074 pairs of instruction-mask sequences derived from 1,042 diverse videos. In contrast to traditional referring video segmentation datasets, such as Ref-YouTube-VOS [37] and MeViS [8], which primarily contain explicit short phrases, ReVOS includes text instructions that necessitate a sophisticated understanding of both video

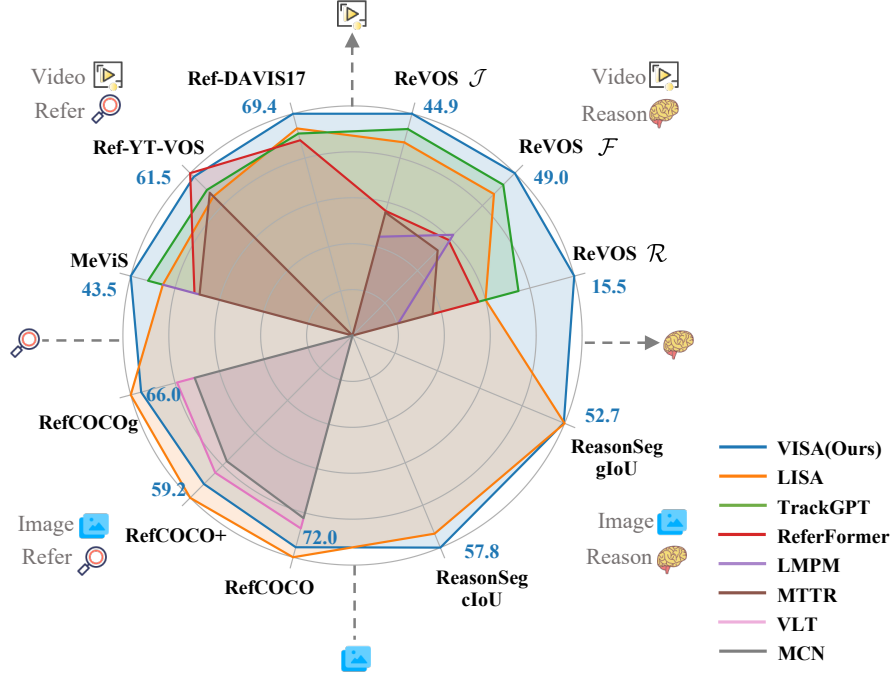


Figure 2. Our proposed VISA consistently achieves state-of-the-art performances on video and image datasets over reasoning and referring segmentation tasks. \mathcal{J} is region similarity [37], \mathcal{F} is contour accuracy [37], and \mathcal{R} is robustness score [20].

content and general world knowledge. We carry out comprehensive experiments on the ReVOS dataset as well as on seven existing segmentation datasets. The results in Fig. 2 demonstrate that VISA not only facilitates advanced reasoning segmentation in both video and image domains but also achieves competitive performance on referring segmentation tasks.

Our main contributions could be summarized as follows: (i) We introduce a new task ReasonVOS (Reasoning Video Object Segmentation), which aims to segment and track objects in videos given implicit texts. ReasonVOS emphasizes the requirements of reasoning, summary, and inference ability based on video content and world knowledge, crucial for an intelligent perception system to interact with dynamic environments. (ii) We propose VISA (Video-based large language Instructed Segmentation Assistant), which efficiently integrates long-term video features and complex text queries to enable the reasoning video object segmentation ability. (iii) We collect a large-scale dataset ReVOS, comprising 1,042 videos and 35,074 object descriptions for instruction tuning and evaluation purposes of ReasonVOS models. The experiments on ReVOS and existing datasets show that our proposed VISA performs robustly in reasoning segmentation tasks of both image and video domains.

2. Related Work

Video Object Segmentation. Video Object Segmentation (VOS) is designed to segment and track objects in

videos based on specific references, including categories [3, 44, 48, 55–58], segmentation masks [4, 6, 30, 32], or explicit text descriptions [2, 8, 22, 37, 47]. VOS plays a critical role in structured video representation learning and Embodied AI. Category-based VOS methods (or Video Instance Segmentation), such as Mask2Former [3], SeqFormer [48], and VisTR [44], segment and associate objects in videos given a pre-defined category list. Mask-based VOS methods (or semi-supervised VOS), such as STM [30] and XMem [4], segment and track objects in videos based on the segmentation mask given in certain frames. The utility of the aforementioned approaches is constrained by their reliance on structured and straightforward input, resulting in limited generalizability in real-world scenarios that necessitate complex reasoning and flexible input formulation.

In contrast, the text-based VOS (Referring VOS) [2, 8, 37], aims to segment objects in videos given text description. However, the text descriptions in Referring VOS fall into short phrases indicating the explicit object information, such as action, localization, and appearance. This system lacks the ability to handle complex sentences that involve common sense reasoning or inference based on video content. In this work, we introduce ReasonVOS, extending the short phrases to complex sentences requiring reasoning and the inference of world knowledge alongside video content. This advancement significantly enhances the practical utility of VOS across various tasks.

Multi-Modal Large Language Model. Inspired by the im-

pressive reasoning capabilities of Large Language Models (LLMs), researchers are investigating methods to transpose these abilities into the vision domain, leading to the development of multi-modal LLMs [1, 43, 54]. Flamingo [1] utilizes a cross-attention structure to attend to visual contexts, facilitating visual in-context learning. Meanwhile, models like BLIP-2 [19] and mPLUG-OWL [51] propose the encoding of image features using a visual encoder, which are subsequently integrated into the LLM along with text embeddings. Otter [18] further incorporates robust few-shot capabilities through in-context instruction tuning on the proposed MIMIC-IT dataset. LLaVA [24] and MiniGPT-4 [59] first conduct image-text feature alignment followed by instruction tuning and also investigate image retrieval for LLMs.

Recent studies have delved into the confluence of multi-modal Large Language Models (LLMs) and vision tasks. VisionLLM [41] provides a versatile interface for engaging with various vision-centric tasks through instruction tuning but fails to fully exploit LLMs for complex reasoning. Kosmos-2 [31] builds a large-scale dataset of grounded image-text pairs, thereby injecting grounding capabilities into LLMs. DetGPT [33] connects the multi-modal LLMs and open-vocabulary detectors, facilitating detection tasks based on user instructions. GPT4RoI [53] innovates by incorporating spatial boxes as input and training the model on region-text pairings. LISA [17] efficiently enables segmentation capabilities of multi-modal LLMs in the image domain by introducing a special $\langle \text{SEG} \rangle$ token. All the above-mentioned methods focus on downstream tasks in the image domain. The concurrent work TrackGPT [38], made the first attempt to tackle reasoning segmentation in videos. However, TrackGPT processes single frames at one time and segments the objects frame-by-frame without any temporal correspondence, which falls in complex scenarios requiring long-term video understanding. On the contrary, our proposed VISA handles multiple frames at one time to obtain long-term awareness.

Video Multi-Modal Large Language Model. To support video understanding in LLMs, Video-LLaMA [52] attempts to utilize BLIP-2 for video embedding extraction, while Video-ChatGPT [27] proposes spatial and temporal pooling for video features. However, given the substantial number of tokens required for each frame, LLMs encounter significant challenges when processing extensive video sequences. It prevents previous work [27, 52] from representing long video sequences that exceed a duration of one hour in LLMs. To solve the issue, LLaMA-VID [21] proposes to efficiently encode each frame with only 2 tokens, which supports long video understanding in existing LLMs. Those works either use pooling or projection to abstract each frame into a few visual tokens, which is inadequate to provide detailed spatial information for segmentation. In

this work, we first select significant frames for identifying the target objects and simultaneously process the selected frames with a large number of visual tokens, avoiding the spatial pooling or projection and thus benefiting the segmentation tasks.

3. Method

3.1. Task Setting

In this section, we start by defining the task of interest, termed ReasonVOS. Specifically, given a high-level query text instruction \mathbf{x}_t for which reasoning with world knowledge is required, and an input video \mathbf{x}_v , we aim to build a model $\varphi_\theta(\cdot)$ that outputs a binary mask sequence \mathcal{M} representing the described object in the input video:

$$\mathcal{M} = \varphi_\theta(\mathbf{x}_t, \mathbf{x}_v), \quad (1)$$

where the input video $\mathbf{x}_v = \{f_t\}_{t=1}^T \in \mathbb{R}^{T \times H \times W \times 3}$ contains T frames, and each frame f_t has a size of $H \times W$. The output binary mask sequence $\mathcal{M} = \{m_t\}_{t=1}^T \in \mathbb{R}^{T \times H \times W}$ has the same frame number and size.

ReasonVOS shares a similar formulation of input and output with the Referring VOS [37] but is far more challenging. The principal difference stems from the complexity of the query text in ReasonVOS. Unlike simple phrases in Referring VOS that directly describe the appearance, action, or localization characteristics (e.g., “*the running car*”), the query texts in ReasonVOS involve more complex expressions that require world knowledge and common sense (e.g., “*the car powered by electricity*”) or expressions that require complex understanding and inference about video content and upcoming events (e.g., “*Which car is most likely to win the race?*”).

3.2. Architecture of VISA

Overview. As shown in Fig. 3, VISA consists of three main components, namely Text-guided Frame Sampler, multi-modal Large Language Model (LLM), and Object Tracker. Specifically, (a) the input video \mathbf{x}_v is fed to the Text-guided Frame Sampler (TFS), which outputs a target frame f_{tgt} for segmentation and T_r corresponding reference frames \mathbf{x}_r to gain long-term information, guided by the text instructions \mathbf{x}_t . (b) Then the selected frames are fed into the multi-modal LLM, generating text output including a special token $\langle \text{SEG} \rangle$ for segmentation of the target frame f_{tgt} . (c) Finally, an Object Tracker is utilized to generate the segmentation masks of all frames \mathcal{M} via bi-directional mask propagation.

Text-guided Frame Sampler. Given input video \mathbf{x}_v comprising T frames where each frame is represented by L visual tokens, the total number of tokens to be processed by the multi-modal LLM is $T \times L$. For segmentation purposes, L should be large enough to maintain spatial de-

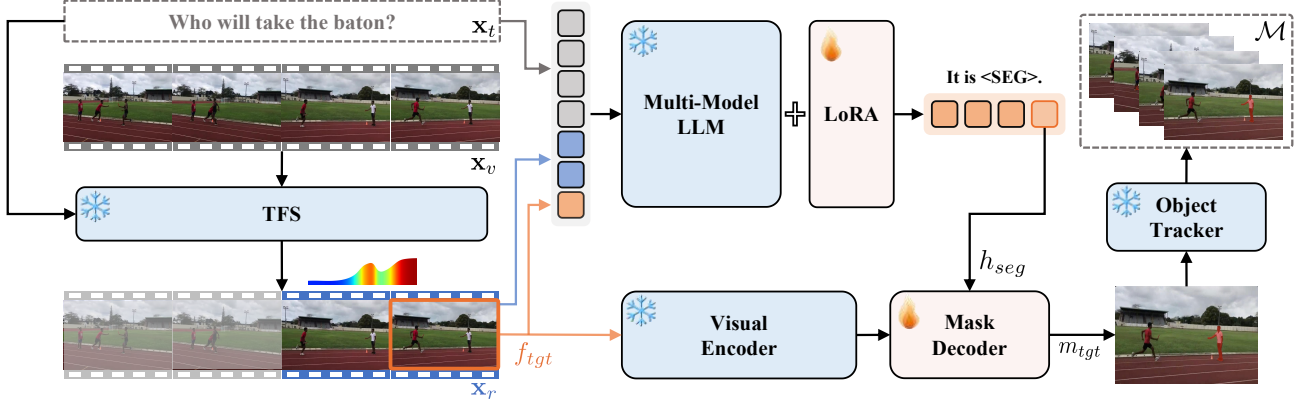


Figure 3. Overview of VISA. (a) Given a video \mathbf{x}_v and a text description \mathbf{x}_t , a Text-guided Frame Sampler (TFS) is proposed to sample the most distinguishing frame f_{tgt} as the target to be segmented and corresponding reference frames \mathbf{x}_r . (b) Then f_{tgt} , \mathbf{x}_r , and \mathbf{x}_t are tokenized and fed to a Multi-Modal LLM to generate text output, including a special token $\langle \text{SEG} \rangle$. The last-layer embedding of $\langle \text{SEG} \rangle$ token h_{seg} is then decoded into the segmentation mask m_{tgt} of frame f_{tgt} via the mask decoder. (c) Finally, the segmentation masks of all frames \mathcal{M} are generated by propagation with an Object Tracker. The modules in blue are frozen during the training, while the modules in pink are trainable.

tails, instead of pooling into a few tokens such as in Video-ChatGPT [27]. Consequently, it is computationally intractable to directly feed such numerous visual tokens to the multi-modal LLM.

As shown in Fig. 3, the text query “Which person will take the baton?” could be answered within the last few frames of the video, while the rest frames are irrelevant to the question. Inspired by this, we adopt LLaMA-VID [21], a multi-modal LLM that abstracts each input frame into two visual tokens and enables long video processes, to serve as a Text-guided Frame Sampler (TFS). TFS generates the most distinguishing frame f_{tgt} and corresponding reference frames \mathbf{x}_r for identifying the described object. Specifically, a task-specific template is designed: “ $\langle \text{VIDEO} \rangle$ To find {description}, which percentage mark of the video should I check? Please respond with a number between 0% and 100%.” We extract the percentage values p_i in the top K responses and use the average value to obtain the target frame $f_{tgt} = f_{T/K \sum p_i}$. K is set to 10 in this work. Based on f_{tgt} , T_r frames are sampled as reference frames \mathbf{x}_r to obtain long-term temporal correspondence and help with the segmentation of the described object in frame f_{tgt} . We adopt multiple reference sampling strategies in this work, such as Local sampling and Global sampling. The details and ablation studies of different reference sampling strategies are shown in Ablation Study Sec. 4.4.

Multi-Modal Large Language Model. Each frame in \mathbf{x}_r and f_{tgt} are encoded via ViT [12] and tokenized into L visual embeddings by Spatial Merging [14], yielding visual tokens $\langle \mathbf{x}_r \rangle$ and $\langle f_{tgt} \rangle$. Then, the concatenated visual and text tokens are fed to a Multi-Modal LLM to generate the text output containing a special token $\langle \text{SEG} \rangle$. The task-specific template is designed as: “USER: $\langle f_{tgt} \rangle$

$\langle \mathbf{x}_r \rangle$ Can you segment the {description}? ASSISTANT: Yes, it is $\langle \text{SEG} \rangle$.”, where {description} will be replaced by the text description, and the text will be tokenized before being fed to multi-modal LLMs. We extract the last-layer embedding corresponding to the $\langle \text{SEG} \rangle$ token and apply an MLP projection layer to generate h_{seg} , which serves as the prompt embedding in SAM decoder [16].

Simultaneously, the vision backbone \mathcal{E}_v extracts the visual features of target frame f_{tgt} , which is utilized along with the prompt embedding h_{seg} to produce the segmentation mask m_{tgt} :

$$m_{tgt} = \text{SAM}(\mathcal{E}_v(f_{tgt}), h_{seg}). \quad (2)$$

Finally, an Object Tracking method [4] is adopted to propagate m_{tgt} bidirectionally to all rest frames and obtain the mask sequence \mathcal{M} :

$$\mathcal{M} = \{m_t\}_{t=1}^T = \text{OT}(m_{tgt}, \mathbf{x}_v). \quad (3)$$

Training. Following LISA [17], our model is trained end-to-end using the standard text generation loss \mathcal{L}_{txt} and the segmentation mask loss $\mathcal{L}_{\text{mask}}$. The overall objective \mathcal{L} is the weighted sum of \mathcal{L}_{txt} and $\mathcal{L}_{\text{mask}}$:

$$\mathcal{L} = \lambda_{\text{txt}} \mathcal{L}_{\text{txt}} + \lambda_{\text{mask}} \mathcal{L}_{\text{mask}}. \quad (4)$$

Specifically, \mathcal{L}_{txt} is the auto-regressive cross-entropy loss for text generation, and $\mathcal{L}_{\text{mask}}$ is the combination of pixel binary cross-entropy (BCE) loss and DICE loss [29], with corresponding loss weights λ_{bce} and λ_{dice} . Given the ground-truth targets ($\hat{\mathbf{y}}_{\text{txt}}$, \hat{m}_{tgt}) and the predictions (\mathbf{y}_{txt} , m_{tgt}), \mathcal{L}_{txt} and $\mathcal{L}_{\text{mask}}$ can be formulated as:

$$\mathcal{L}_{\text{txt}} = \text{CE}(\hat{\mathbf{y}}_{\text{txt}}, \mathbf{y}_{\text{txt}}), \quad (5)$$

$$\mathcal{L}_{\text{mask}} = \lambda_{\text{bce}} \text{BCE}(\hat{m}_{tgt}, m_{tgt}) + \lambda_{\text{dice}} \text{DICE}(\hat{m}_{tgt}, m_{tgt}). \quad (6)$$

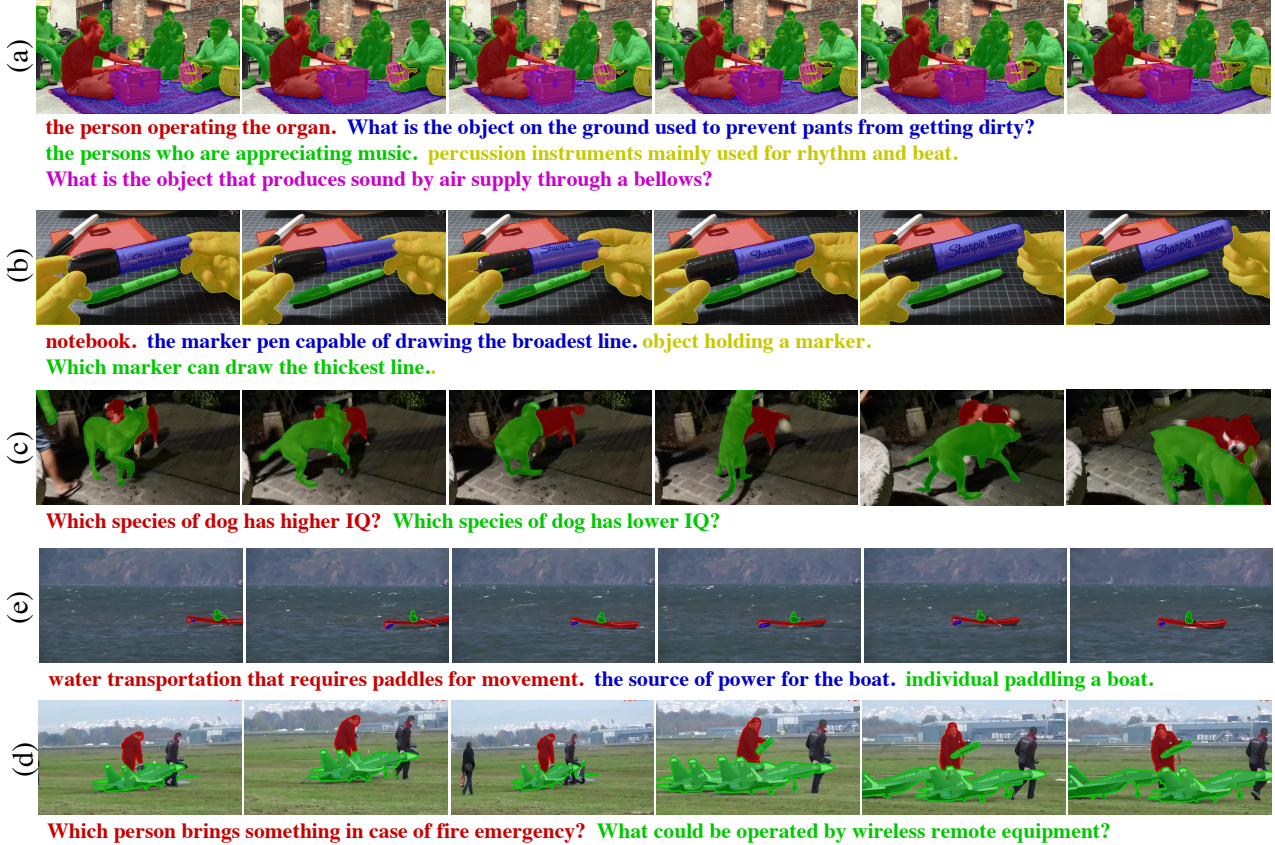


Figure 4. Visualizations of VISA on ReVOS dataset.

3.3. ReVOS Dataset

For the quantitative evaluation of ReasonVOS, it is essential to establish a benchmark characterized by implicit object descriptions and high-quality mask sequences. To this end, we collect ReVOS, a dataset containing complex text instructions and corresponding high-quality masks in videos for both instruction tuning and evaluation of ReasonVOS. To guarantee reliable assessment, we collect a diverse set of videos from LV-VIS [39, 40], MOSE [9], OVIS [35], TAO [7] and UVO [42]. Subsequently, we annotate the objects in the videos with complex text instructions and match these instructions with the corresponding target mask sequences.

Dataset Statistics Overall, our dataset comprises a total of 35,074 object-instruction pairs from 1,042 videos. All the videos are divided into a training (instruction tuning) set and a validation set containing 626 videos and 416 videos respectively. The text instructions consist of (1) 14,678 implicit descriptions requiring world knowledge and video content reasoning and inference to evaluate the ReasonVOS; (2) 20,071 explicit descriptions to evaluate the generalization ability in traditional Referring VOS task; (3) 325 descriptions of nonexistent objects for the hallu-

cination evaluation. Check <https://github.com/cilinyan/ReVOS-api> for more detailed dataset information.

Evaluation Metrics We follow most previous works on Referring VOS [8, 37] to adopt \mathcal{J} & \mathcal{F} as the main evaluation metric, which is the average of region similarity \mathcal{J} and contour accuracy \mathcal{F} . As for the evaluation of hallucination, we adopt the robustness score \mathcal{R} introduced in R2VOS [20].

4. Experiments

4.1. Dataset

Training Dataset. Our training data consists of vanilla Referring VOS datasets, Video Question-Answering datasets, Image datasets, and the ReVOS dataset. The details are as follows: (1) Referring VOS datasets. We use Ref-YouTubeVOS [37], MeViS [8], and Ref-DAVIS17 [34] during training to learn the projections between objects in videos and text expressions. Those Referring VOS datasets provide input videos, explicit short descriptions, and corresponding object masks. (2) Video Question-Answering datasets. To achieve better reasoning and question-answering ability in videos of the multi-modal LLM, we include the video instruction data from Video-ChatGPT [27]. The answer tem-

plate “It’s <SEG>” is replaced by the original annotated answers in those datasets, and the corresponding segmentation loss is ignored during training. (3) Image datasets. Images could be regarded as one-frame videos. Thereby, we adopt all the vanilla datasets used by LISA [17] in our work to achieve more stable training. (4) ReVOS dataset. The above-mentioned training datasets contain no ReasonVOS samples. Therefore, we include the ReVOS dataset during training to achieve more comprehensive reasoning and object segmentation ability in videos. The implementation details are shown in Supplementary Material.

Evaluation Dataset We evaluate VISA on both Video datasets and Image datasets. (1) Video datasets. We use the ReVOS dataset to evaluate the performance of ReasonVOS; we use Ref-YouTube-VOS [37], MeViS [8], and Ref-DAVIS17 [34] to evaluate the performance of vanilla Referring VOS. (2) Image datasets. We use ReasonSeg [17], refCOCO [15], refCOCO+ [15], and refCOCOg [28] to evaluate the generalization ability of VISA on image-level segmentation tasks.

4.2. Implementation Details

We adopt the decoder in SAM [16] as the segmentation decoder. We choose Chat-UniVi-7B and Chat-UniVi-13B [14] as the pre-trained Multi-Modal LLM. The number of visual tokens L per frame is set to 112, the same as the number in Chat-UniVi. We utilize XMem [4], a semi-supervised Video Object Segmentation method as the Object Tracker. The Text-guided Frame Sampler, Visual Backbone, and Object Tracker are all frozen during the training. Only the multi-modal LLM and SAM decoders are trainable. We leverage LoRA [13] to perform efficient fine-tuning of the multi-modal LLM. During training, we randomly sample a target frame f_{tgt} and 8-12 reference frames \mathbf{x}_t per video instead of using the Text-guided Frame Sampler, to achieve more comprehensive training. During inference, we use the Text-guided Frame Sampler to obtain f_{tgt} and 12 reference frames \mathbf{x}_t with the Global-Local sampling strategy. We use 8 NVIDIA 80G A100 GPUs for training. The training scripts are based on the deepspeed [36] engine. We train VISA for 10 epochs with a batch size of 128. Specifically, the batch size per device is set to 1, and the gradient accumulation step is set to 16, leading to 128 samples on 8 GPUs in total. We employ the AdamW [25] optimizer with a cosine schedule. The learning rate is set to $2e-5$. All input frames are resized to 224×224 before feeding into the LLM, while the frame for the segmentation branch is resized to 1024×1024 . The weights of the text generation loss λ_{txt} and the mask loss λ_{mask} are set to 1.0 and 1.0, respectively. The weights of the binary cross-entropy loss λ_{bce} and the dice loss λ_{dice} are set to 2.0 and 0.5, respectively. Check <https://github.com/cilinyan/VISA> for more implementation details.

4.3. Comparison

ReVOS. The results comparison on ReVOS are shown in Tab. 1. Compared with traditional methods (even with extremely large visual backbones), our proposed VISA(IT)-7B generally achieves over 20 $\mathcal{J}\&\mathcal{F}$ improvements in terms of reasoning. Those traditional works are limited to short explicit references and have no capability of reasoning and understanding the implicit text queries.

VISA(IT)-7B outperforms the single frame method LISA-7B [17] by 6.0 $\mathcal{J}\&\mathcal{F}$ in terms of overall performance, which indicates the ability of VISA to conduct video-level segmentation. Recent work TrackGPT [38] incorporates tracking with LLMs, yet the multi-modal LLMs in TrackGPT only process a single frame at one time, leading to poor temporal information gathering. As a consequence, VISA(IT)-7B outperforms TrackGPT(IT)-7B by 3.3 $\mathcal{J}\&\mathcal{F}$ overall. Moreover, as we include plenty of negative samples (text queries of nonexistent objects) in the ReVOS training set, the hallucination of VISA is much lower than in existing methods. As shown, the robustness scores \mathcal{R} of VISA are much higher than existing methods.

VQA+ReferringVOS could serve as a baseline model, but can not solve ReasonVOS well. As suggested in Tab. 1, we use LLaMA-VID, a Video-VQA method, to transfer the complex questions (e.g., scared dog) into low-level descriptions (e.g., dog on left), and then employ LMPM, a RVOS method, to segment the described objects. As shown below, LLaMA-VID + LMPM performs worse than LMPM on ReVOS reasoning set. That is because the existing video-VQA methods take only a few visual tokens per frame, which is too vague to localize the described objects and brings mistakes when converting complex questions into low-level expressions.

Note that VISA with LLaVA-7B [24] and Chat-UniVi-7B [14] achieve similar performance. Chat-UniVi could process a flexible number of visual tokens via spatial merging, thus we chose it in this work. We visualize the results of VISA on the ReVOS dataset in Fig. 4.

Referring VOS. To demonstrate that VISA generalizes well in the vanilla Referring VOS task, we compare VISA with the existing methods in Tab. 2. As shown, VISA achieves the SOTA results over three widely used Referring VOS datasets.

Image Datasets. Images could be regarded as single-frame videos. Therefore, VISA could be directly applied to image datasets without any modification. As shown in Tab. 3, VISA achieves comparable performance with LISA on three referring image segmentation datasets, while significantly outperforming traditional methods by over 20% on the ReasonSeg [17] dataset. The results indicate that VISA has a strong generalization ability on vanilla referring image segmentation and reasoning image segmentation.

Table 1. Performance comparison on ReVOS dataset. * means the method is reproduced in this work. (IT) means instruction tuning with the ReVOS training set. \mathcal{R} is the robustness score.

Method	Backbone	referring			reasoning			overall			\mathcal{R}
		\mathcal{J}	\mathcal{F}	$\mathcal{J}\&\mathcal{F}$	\mathcal{J}	\mathcal{F}	$\mathcal{J}\&\mathcal{F}$	\mathcal{J}	\mathcal{F}	$\mathcal{J}\&\mathcal{F}$	
ReferFormer [47]	Resnet50	16.6	17.1	16.9	11.9	13.8	12.8	14.3	15.4	14.9	4.9
MTTR [2]	Video-Swin-T	29.8	30.2	30.0	20.4	21.5	21.0	25.1	25.9	25.5	5.6
LMPM [8]	Swin-T	29.0	39.1	34.1	13.3	24.3	18.8	21.2	31.7	26.4	3.2
ReferFormer [47]	Video-Swin-B	31.2	34.3	32.7	21.3	25.6	23.4	26.2	29.9	28.1	8.8
LLaMA-VID [21]+LMPM	Swin-T	29.0	39.1	34.1	12.8	23.7	18.2	20.9	31.4	26.1	3.4
LISA [17]	LLaVA-7B	44.3	47.1	45.7	33.8	38.4	36.1	39.1	42.7	40.9	9.3
LISA* [17]	LLaVA-13B	45.2	47.9	46.6	34.3	39.1	36.7	39.8	43.5	41.6	8.6
TrackGPT(IT)* [38]	LLaVA-7B	46.7	49.7	48.2	36.8	41.2	39.0	41.8	45.5	43.6	11.6
TrackGPT(IT)* [38]	LLaVA-13B	48.3	50.6	49.5	38.1	42.9	40.5	43.2	46.8	45.0	12.8
VISA	Chat-UniVi-7B	51.1	54.7	52.9	36.7	41.7	39.2	43.9	48.2	46.1	7.9
VISA	Chat-UniVi-13B	52.3	55.8	54.1	38.3	43.5	40.9	45.3	49.7	47.5	8.3
VISA(IT)	LLaVA-7B	49.4	52.6	51.0	40.5	45.8	43.2	44.9	49.2	47.1	<u>15.3</u>
VISA(IT)	LLaVA-13B	55.7	<u>59.0</u>	57.4	<u>41.9</u>	<u>46.5</u>	<u>44.2</u>	48.8	<u>52.8</u>	<u>50.8</u>	15.1
VISA(IT)	Chat-UniVi-7B	49.2	52.6	50.9	40.6	45.4	43.0	44.9	49.0	46.9	15.5
VISA(IT)	Chat-UniVi-13B	<u>55.6</u>	59.1	57.4	42.0	46.7	44.3	48.8	52.9	50.9	14.5

Table 2. Performance comparison on Referring VOS datasets. The results on MeViS above the horizontal line are provided in LMPM [8], which are all obtained with the Swin-T backbone. The results of TrackGPT on MeViS are generated by our reproduced model.

Methods	Backbone	MeViS			Ref-YT-VOS			Ref-DAVIS17		
		\mathcal{J}	\mathcal{F}	$\mathcal{J}\&\mathcal{F}$	\mathcal{J}	\mathcal{F}	$\mathcal{J}\&\mathcal{F}$	\mathcal{J}	\mathcal{F}	$\mathcal{J}\&\mathcal{F}$
URVOS [37]	ResNet50	25.7	29.9	27.8	45.3	49.2	47.2	47.3	56.0	51.6
LBDT [11]	ResNet50	27.8	30.8	29.3	48.2	50.6	49.4	-	-	54.1
MTTR [2]	Video-Swin-T	28.8	31.2	30.0	54.0	56.6	55.3	-	-	-
ReferFormer [47]	Video-Swin-B	29.8	32.2	31.0	61.3	64.6	62.9	58.1	64.1	61.1
LMPM [8]	Swin-T	34.2	40.2	37.2	-	-	-	-	-	-
OnlineRefer [46]	Swin-L	-	-	-	61.6	65.5	63.5	61.6	67.7	64.8
LISA [17]	LLaVA-7B	35.1	39.4	37.2	53.4	54.3	53.9	62.2	67.3	64.8
LISA [17]	LLaVA-13B	35.8	40.0	37.9	54.0	54.8	54.4	63.2	68.8	66.0
TrackGPT [38]	LLaVA-7B	37.6	42.6	40.1	55.3	57.4	56.4	59.4	67.0	63.2
TrackGPT [38]	LLaVA-13B	39.2	43.1	41.2	58.1	60.8	59.5	62.7	70.4	66.5
VISA (Ours)	Chat-UniVi-7B	<u>40.7</u>	<u>46.3</u>	<u>43.5</u>	59.8	63.2	61.5	<u>66.3</u>	<u>72.5</u>	<u>69.4</u>
VISA (Ours)	Chat-UniVi-13B	41.8	47.1	44.5	<u>61.4</u>	<u>64.7</u>	<u>63.0</u>	67.0	73.8	70.4

4.4. Ablation Studies

Training Datasets In Tab. 4, we show the contribution of each type of dataset during training. As shown, without Referring VOS datasets, the performance drops by 3.3% $\mathcal{J}\&\mathcal{F}$ and 3.1% $\mathcal{J}\&\mathcal{F}$ in terms of referring and reasoning segmentation, respectively. That is because Referring VOS datasets provide text expressions and mask sequence pairs in videos, aligning the video domain and linguistic domain, thus generally helping with the vanilla referring segmentation and reasoning segmentation tasks in videos. With-

out Image datasets, the performance of VISA significantly drops by 16.7% and 9.5%. Generally, image datasets have much larger scales than video datasets, leading to more robust feature alignment and stronger generalization ability. The models tend to be overfitting during training without image datasets. By instruction tuning on ReVOS, VISA further gains 3.8% $\mathcal{J}\&\mathcal{F}$ performance improvements of reasoning segmentation, while the performance of referring segmentation barely changes, which shows the effectiveness of our collected ReVOS dataset to improve the complex video reasoning ability.

Table 3. Performance comparison on Image Segmentation datasets. [†] denotes the results obtained from the model we trained via LISA’s official GitHub repository.

Methods	Backbone	refCOCO			refCOCO+			refCOCog		ReasonSeg	
		val	testA	testB	val	testA	testB	val(U)	test(U)	gIoU	cIoU
MCN [26]	Darknet53	62.4	64.2	59.7	50.6	55.0	44.7	49.2	49.4	-	-
VLТ [10]	Darknet53	65.7	68.3	62.7	55.5	59.2	49.4	53.0	56.7	-	-
CRIS [45]	ResNet101	70.5	73.2	66.1	62.3	68.1	53.7	59.9	60.4	-	-
LAVT [49]	Swin-B	72.7	75.8	68.8	62.1	68.4	55.1	61.2	62.1	-	-
ReLA [23]	Swin-B	73.8	76.5	70.2	66.0	71.0	57.7	65.0	66.0	-	-
X-Decoder [60]	DaViT-L	-	-	-	-	-	-	64.6	-	22.6	17.9
SEEM [61]	DaViT-L	-	-	-	-	-	-	65.7	-	25.5	21.2
LISA [17]	LLaVA-7B	74.9	79.1	72.3	65.1	70.8	58.1	67.9	70.6	52.9	54.0
LISA [†]	LLaVA-7B	70.8	73.7	66.3	58.1	63.2	51.2	63.8	64.8	48.1	53.7
VISA (Ours)	Chat-UniVi-7B	72.4	75.5	68.1	59.8	64.8	53.1	65.5	66.4	52.7	57.8

Table 4. Performance on ReVOS validation set with different training datasets. The columns with \checkmark mean the corresponding datasets are adopted during training.

ReferringVOS	VQA	Image	ReVOS	referring			reasoning		
				\mathcal{J}	\mathcal{F}	$\mathcal{J}\&\mathcal{F}$	\mathcal{J}	\mathcal{F}	$\mathcal{J}\&\mathcal{F}$
	\checkmark	\checkmark	\checkmark	45.9	49.3	47.6	37.4	42.3	39.9
\checkmark		\checkmark	\checkmark	48.6	52.1	50.3	38.9	43.9	41.4
\checkmark	\checkmark		\checkmark	32.3	36.2	34.2	30.9	36.1	33.5
\checkmark	\checkmark	\checkmark		51.1	54.7	52.9	36.7	41.7	39.2
\checkmark	\checkmark	\checkmark	\checkmark	49.2	52.6	50.9	40.6	45.4	43.0

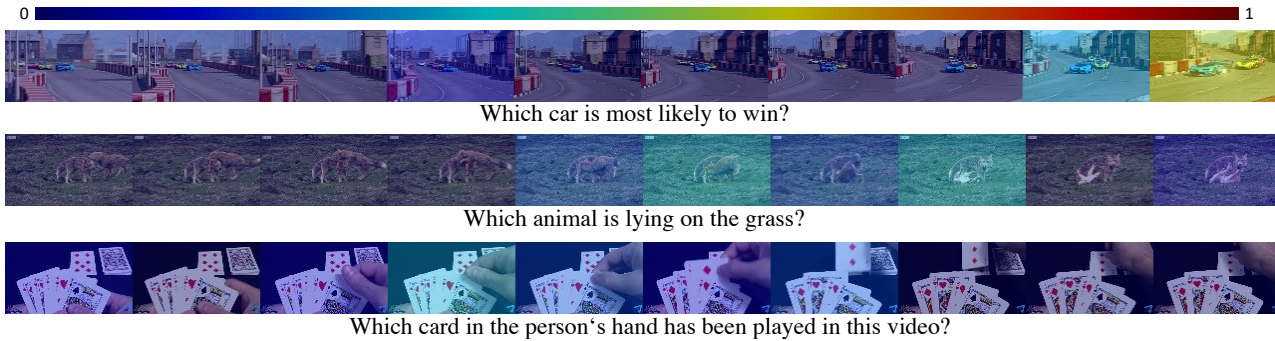


Figure 5. Heatmaps of the target frame f_{tgt} . To draw the heatmap, we generate 10 responses with the Text-guided Frame Sampler (TFS) and obtain the normalized distribution. As shown, the highlighted frames are related to the text queries.

Target Frame f_{tgt} . We visualize the heatmaps of the target frame f_{tgt} in Fig. 5. As shown in the figure, the frames related to given text expressions are highlighted. We show the ablation of f_{tgt} in Tab. 5. f_0 means we directly segment the object in the first frame and propagate to the rest frames, while f_{tgt} means we use TFS to obtain the target frame f_{tgt} and segment f_{tgt} in consequence. As shown, the performance with f_{tgt} generally outperforms f_0 by around 2% under different settings, which indicates the effectiveness of TFS in obtaining the significant moments related to

described objects.

Reference Sampling Strategies. In Tab. 5, Global means we uniformly sample frames through the whole video as reference frames \mathbf{x}_r , while Local means we sample contiguous frames centered by f_{tgt} as reference frames. Global-Local means the combination of $T_r/2$ frames from Global and $T_r/2$ frames from Local. As shown, Global-Local sampling slightly outperforms the separate ones, thus we adopt it in VISA. As the number T_r of reference frames \mathbf{x}_r increases, the performance gradually improves. To keep feasi-

Table 5. Overall $\mathcal{J}\&\mathcal{F}$ on ReVOS with different number T_r of reference frames \mathbf{x}_r and different sampling strategies.

	T_r	w/o Sample	Global	Local	Global-Local
f_0	0	42.6	-	-	-
	6	-	43.9	44.5	44.6
	12	-	44.5	44.9	45.0
f_{tgt}	0	44.3	-	-	-
	6	-	46.0	46.1	46.3
	12	-	46.7	46.3	46.9

Table 6. The performance comparison on ReVOS with different number L of visual tokens per frame.

L	backbone	referring			reasoning		
		\mathcal{J}	\mathcal{F}	$\mathcal{J}\&\mathcal{F}$	\mathcal{J}	\mathcal{F}	$\mathcal{J}\&\mathcal{F}$
256	LLaVA-7B	49.4	52.6	51.0	40.5	45.8	43.2
112	Chat-UniVi-7B	49.2	52.6	50.9	40.6	45.4	43.0
56	Chat-UniVi-7B	44.9	48.5	46.7	36.5	41.5	39.0

ble training and inference, we adopt $T_r=12$ in VISA. Overall, with f_{tgt} and Global-Local sampling, VISA achieves 4.3% $\mathcal{J}\&\mathcal{F}$ improvements on the ReVOS dataset.

Number L of visual tokens. The performance comparison under different numbers L of visual tokens per frame is shown in Tab 6. For $L=256$, we adopt LLaVA-7B [24] as the backbone, which takes 256 visual tokens for the input image. For $L=112$ and $L=52$, we use Chat-UniVi-7B [14] as the backbone, and utilize the Spatial Merging [14] to project visual tokens to corresponding numbers. As shown, VISA with 256 tokens and 112 tokens per frame achieves comparable performance on ReVOS. When L is set to 52, the performance of VISA significantly drops. Therefore, we adopt $L=112$ in this work.

4.5. Limitations

Small Objects Limited by the number of visual tokens per frame (for instance, 256 in LISA [24], and 112 in VISA), the current methods have a poor ability to capture very small objects. As shown in Fig. 4 (d), the small paddles are not segmented. A multi-modal LLM with more input visual tokens could relieve this issue, but will lead to more computational burden and complex training process.

Temporal Information Gathering In this work, we intuitively adopt a Text-guided Frame Sampler to select a feasible number of important frames for the multi-modal LLM. The performance highly relies on the accuracy of located frames. Some objects may only appear in a few frames, which is hard to locate. As shown in Fig. 4 (e), the person with a fire tank only appears in one frame, while VISA falls to locate this frame and segment another person in

consequence. Moreover, the text description could require extremely long temporal correspondence, but VISA could only handle a few selected frames at the same time. To this end, a more effective way to gather long-term temporal information while maintaining spatial details is required. We leave those issues to our future work.

5. Conclusion

In this work, we propose a new task, ReasonVOS, which aims to generate object mask sequences in response to text queries that require complex reasoning and inference abilities within video contexts. To tackle ReasonVOS, we design VISA (Video-based large language Instructed Segmentation Assistant), to leverage the world knowledge and reasoning capabilities of multi-modal LLMs while possessing the ability to segment and track objects in videos. Moreover, we collect a large-scale dataset ReVOS, containing 35,074 expression-mask pairs from 1,042 videos for the instruction tuning and evaluation of ReasonVOS methods. Experiments on eight various datasets show that our proposed VISA not only enables the reasoning segmentation ability in videos but also generally provides SOTA performance on traditional video and image segmentation tasks.

Acknowledgement

This project is supported by National Natural Science Foundation of China under Grant 92370114 and European Union (ERC, EVA, 950086).

References

- [1] Jean-Baptiste Alayrac, Jeff Donahue, Pauline Luc, Antoine Miech, Iain Barr, Yana Hasson, Karel Lenc, Arthur Mensch, Katherine Millican, Malcolm Reynolds, et al. Flamingo: a visual language model for few-shot learning. *Advances in Neural Information Processing Systems*, 35:23716–23736, 2022. 4
- [2] Adam Botach, Evgenii Zheltonozhskii, and Chaim Baskin. End-to-end referring video object segmentation with multi-modal transformers. In *Proceedings of the IEEE/CVF Conference on Computer Vision and Pattern Recognition*, pages 4985–4995, 2022. 1, 3, 8
- [3] Bowen Cheng, Anwesa Choudhuri, Ishan Misra, Alexander Kirillov, Rohit Girdhar, and Alexander G Schwing. Mask2former for video instance segmentation. *arXiv preprint arXiv:2112.10764*, 2021. 1, 3
- [4] Ho Kei Cheng and Alexander G Schwing. Xmem: Long-term video object segmentation with an atkinson-shiffrin memory model. In *European Conference on Computer Vision*, pages 640–658. Springer, 2022. 2, 3, 5, 7
- [5] Ho Kei Cheng, Yu-Wing Tai, and Chi-Keung Tang. Rethinking space-time networks with improved memory coverage for efficient video object segmentation. *Advances in Neural Information Processing Systems*, 34:11781–11794, 2021. 1

- [6] Jingchun Cheng, Yi-Hsuan Tsai, Wei-Chih Hung, Shengjin Wang, and Ming-Hsuan Yang. Fast and accurate online video object segmentation via tracking parts. In *Proceedings of the IEEE conference on computer vision and pattern recognition*, pages 7415–7424, 2018. 3
- [7] Achal Dave, Tarasha Khurana, Pavel Tokmakov, Cordelia Schmid, and Deva Ramanan. Tao: A large-scale benchmark for tracking any object. In *Computer Vision–ECCV 2020: 16th European Conference, Glasgow, UK, August 23–28, 2020, Proceedings, Part V 16*, pages 436–454. Springer, 2020. 6
- [8] Henghui Ding, Chang Liu, Shuting He, Xudong Jiang, and Chen Change Loy. Mevis: A large-scale benchmark for video segmentation with motion expressions. In *Proceedings of the IEEE/CVF International Conference on Computer Vision*, pages 2694–2703, 2023. 2, 3, 6, 7, 8
- [9] Henghui Ding, Chang Liu, Shuting He, Xudong Jiang, Philip HS Torr, and Song Bai. Mose: A new dataset for video object segmentation in complex scenes. *arXiv preprint arXiv:2302.01872*, 2023. 6
- [10] Henghui Ding, Chang Liu, Suchen Wang, and Xudong Jiang. Vision-language transformer and query generation for referring segmentation. In *Proceedings of the IEEE/CVF International Conference on Computer Vision*, pages 16321–16330, 2021. 9
- [11] Zihan Ding, Tianrui Hui, Junshi Huang, Xiaoming Wei, Jizhong Han, and Si Liu. Language-bridged spatial-temporal interaction for referring video object segmentation. In *Proceedings of the IEEE/CVF Conference on Computer Vision and Pattern Recognition*, pages 4964–4973, 2022. 8
- [12] Alexey Dosovitskiy, Lucas Beyer, Alexander Kolesnikov, Dirk Weissenborn, Xiaohua Zhai, Thomas Unterthiner, Mostafa Dehghani, Matthias Minderer, Georg Heigold, Sylvain Gelly, et al. An image is worth 16x16 words: Transformers for image recognition at scale. *arXiv preprint arXiv:2010.11929*, 2020. 5
- [13] Edward J Hu, Yelong Shen, Phillip Wallis, Zeyuan Allen-Zhu, Yuanzhi Li, Shean Wang, Lu Wang, and Weizhu Chen. Lora: Low-rank adaptation of large language models. *arXiv preprint arXiv:2106.09685*, 2021. 7
- [14] Peng Jin, Ryuichi Takanobu, Caiwan Zhang, Xiaochun Cao, and Li Yuan. Chat-univi: Unified visual representation empowers large language models with image and video understanding. *arXiv preprint arXiv:2311.08046*, 2023. 5, 7, 10
- [15] Sahar Kazemzadeh, Vicente Ordonez, Mark Matten, and Tamara Berg. Referitgame: Referring to objects in photographs of natural scenes. In *Proceedings of the 2014 conference on empirical methods in natural language processing (EMNLP)*, pages 787–798, 2014. 7
- [16] Alexander Kirillov, Eric Mintun, Nikhila Ravi, Hanzi Mao, Chloe Rolland, Laura Gustafson, Tete Xiao, Spencer Whitehead, Alexander C Berg, Wan-Yen Lo, et al. Segment anything. *arXiv preprint arXiv:2304.02643*, 2023. 2, 5, 7
- [17] Xin Lai, Zhuotao Tian, Yukang Chen, Yanwei Li, Yuhui Yuan, Shu Liu, and Jiaya Jia. Lisa: Reasoning segmentation via large language model. *arXiv preprint arXiv:2308.00692*, 2023. 1, 2, 4, 5, 7, 8, 9
- [18] Bo Li, Yuanhan Zhang, Liangyu Chen, Jinghao Wang, Jingkang Yang, and Ziwei Liu. Otter: A multi-modal model with in-context instruction tuning. *arXiv preprint arXiv:2305.03726*, 2023. 4
- [19] Junnan Li, Dongxu Li, Silvio Savarese, and Steven Hoi. Blip-2: Bootstrapping language-image pre-training with frozen image encoders and large language models. *arXiv preprint arXiv:2301.12597*, 2023. 4
- [20] Xiang Li, Jinglu Wang, Xiaohao Xu, Xiao Li, Yan Lu, and Bhiksha Raj. R²vos: Robust referring video object segmentation via relational multimodal cycle consistency. *arXiv preprint arXiv:2207.01203*, 2022. 3, 6
- [21] Yanwei Li, Chengyao Wang, and Jiaya Jia. Llama-vid: An image is worth 2 tokens in large language models. *arXiv preprint arXiv:2311.17043*, 2023. 4, 5, 8
- [22] Zhenyang Li, Ran Tao, Efstratios Gavves, Cees G. M. Snoek, and Arnold W. M. Smeulders. Tracking by natural language specification. In *2017 IEEE Conference on Computer Vision and Pattern Recognition (CVPR)*, pages 7350–7358, 2017. 3
- [23] Chang Liu, Henghui Ding, and Xudong Jiang. Gres: Generalized referring expression segmentation. In *Proceedings of the IEEE/CVF Conference on Computer Vision and Pattern Recognition*, pages 23592–23601, 2023. 9
- [24] Haotian Liu, Chunyuan Li, Qingyang Wu, and Yong Jae Lee. Visual instruction tuning. *Advances in neural information processing systems*, 36, 2024. 4, 7, 10
- [25] Ilya Loshchilov and Frank Hutter. Decoupled weight decay regularization. *arXiv preprint arXiv:1711.05101*, 2017. 7
- [26] Gen Luo, Yiyi Zhou, Xiaoshuai Sun, Liujuan Cao, Chenglin Wu, Cheng Deng, and Rongrong Ji. Multi-task collaborative network for joint referring expression comprehension and segmentation. In *Proceedings of the IEEE/CVF Conference on computer vision and pattern recognition*, pages 10034–10043, 2020. 9
- [27] Muhammad Maaz, Hanoona Rasheed, Salman Khan, and Fahad Shahbaz Khan. Video-chatgpt: Towards detailed video understanding via large vision and language models. *arXiv preprint arXiv:2306.05424*, 2023. 4, 5, 6
- [28] Junhua Mao, Jonathan Huang, Alexander Toshev, Oana Camburu, Alan L Yuille, and Kevin Murphy. Generation and comprehension of unambiguous object descriptions. In *Proceedings of the IEEE conference on computer vision and pattern recognition*, pages 11–20, 2016. 7
- [29] Fausto Milletari, Nassir Navab, and Seyed-Ahmad Ahmadi. V-net: Fully convolutional neural networks for volumetric medical image segmentation. In *2016 fourth international conference on 3D vision*, pages 565–571. IEEE, 2016. 5
- [30] Seoung Wug Oh, Joon-Young Lee, Ning Xu, and Seon Joo Kim. Video object segmentation using space-time memory networks. In *Proceedings of the IEEE/CVF International Conference on Computer Vision*, pages 9226–9235, 2019. 3
- [31] Zhiliang Peng, Wenhui Wang, Li Dong, Yaru Hao, Shaohan Huang, Shuming Ma, and Furu Wei. Kosmos-2: Grounding multimodal large language models to the world. *arXiv preprint arXiv:2306.14824*, 2023. 4
- [32] Federico Perazzi, Anna Khoreva, Rodrigo Benenson, Bernt Schiele, and Alexander Sorkine-Hornung. Learning video

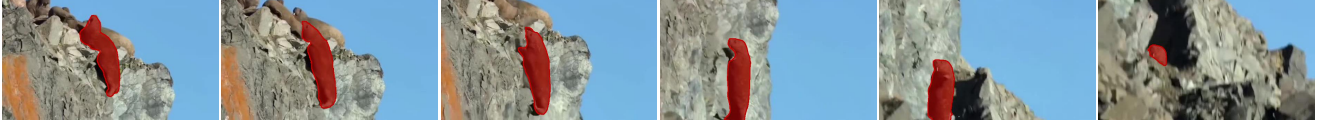
- object segmentation from static images. In *Proceedings of the IEEE conference on computer vision and pattern recognition*, pages 2663–2672, 2017. 3
- [33] Renjie Pi, Jiahui Gao, Shizhe Diao, Rui Pan, Hanze Dong, Jipeng Zhang, Lewei Yao, Jianhua Han, Hang Xu, and Lingpeng Kong Tong Zhang. Detgpt: Detect what you need via reasoning. *arXiv preprint arXiv:2305.14167*, 2023. 4
- [34] Jordi Pont-Tuset, Federico Perazzi, Sergi Caelles, Pablo Arbeláez, Alex Sorkine-Hornung, and Luc Van Gool. The 2017 davis challenge on video object segmentation. *arXiv preprint arXiv:1704.00675*, 2017. 6, 7
- [35] Jiyang Qi, Yan Gao, Yao Hu, Xinggang Wang, Xiaoyu Liu, Xiang Bai, Serge Belongie, Alan Yuille, Philip HS Torr, and Song Bai. Occluded video instance segmentation: Dataset and iccv 2021 challenge. *arXiv preprint arXiv:2111.07950*, 2021. 6
- [36] Jeff Rasley, Samyam Rajbhandari, Olatunji Ruwase, and Yuxiong He. Deepspeed: System optimizations enable training deep learning models with over 100 billion parameters. In *Proceedings of the 26th ACM SIGKDD International Conference on Knowledge Discovery & Data Mining*, pages 3505–3506, 2020. 7
- [37] Seonguk Seo, Joon-Young Lee, and Bohyung Han. Urvos: Unified referring video object segmentation network with a large-scale benchmark. In *Computer Vision–ECCV 2020: 16th European Conference, Glasgow, UK, August 23–28, 2020, Proceedings, Part XV 16*, pages 208–223. Springer, 2020. 1, 2, 3, 4, 6, 7, 8
- [38] Nicholas Stroth. Trackgpt—a generative pre-trained transformer for cross-domain entity trajectory forecasting. *arXiv preprint arXiv:2402.00066*, 2024. 4, 7, 8
- [39] Haochen Wang, Cilin Yan, Keyan Chen, Xiaolong Jiang, Xu Tang, Yao Hu, Guoliang Kang, Weidi Xie, and Efstratios Gavves. Ov-vis: Open-vocabulary video instance segmentation. *International Journal of Computer Vision*, pages 1–18, 2024. 6
- [40] Haochen Wang, Cilin Yan, Shuai Wang, Xiaolong Jiang, Xu Tang, Yao Hu, Weidi Xie, and Efstratios Gavves. Towards open-vocabulary video instance segmentation. In *Proceedings of the IEEE/CVF International Conference on Computer Vision*, pages 4057–4066, 2023. 6
- [41] Wenhai Wang, Zhe Chen, Xiaokang Chen, Jiannan Wu, Xizhou Zhu, Gang Zeng, Ping Luo, Tong Lu, Jie Zhou, Yu Qiao, et al. Visionllm: Large language model is also an open-ended decoder for vision-centric tasks. *Advances in Neural Information Processing Systems*, 36, 2024. 4
- [42] Weiyao Wang, Matt Feiszli, Heng Wang, and Du Tran. Unidentified video objects: A benchmark for dense, open-world segmentation. In *Proceedings of the IEEE/CVF international conference on computer vision*, pages 10776–10785, 2021. 6
- [43] Weihang Wang, Qingsong Lv, Wenmeng Yu, Wenyi Hong, Ji Qi, Yan Wang, Junhui Ji, Zhuoyi Yang, Lei Zhao, Xixuan Song, et al. Cogvlm: Visual expert for pretrained language models. *arXiv preprint arXiv:2311.03079*, 2023. 4
- [44] Yuqing Wang, Zhaoliang Xu, Xinlong Wang, Chunhua Shen, Baoshan Cheng, Hao Shen, and Huaxia Xia. End-to-end video instance segmentation with transformers. In *Proceedings of the IEEE/CVF conference on computer vision and pattern recognition*, pages 8741–8750, 2021. 1, 3
- [45] Zhaoqing Wang, Yu Lu, Qiang Li, Xunqiang Tao, Yandong Guo, Mingming Gong, and Tongliang Liu. Cris: Clip-driven referring image segmentation. In *Proceedings of the IEEE/CVF conference on computer vision and pattern recognition*, pages 11686–11695, 2022. 9
- [46] Dongming Wu, Tiancai Wang, Yuang Zhang, Xiangyu Zhang, and Jianbing Shen. Onlinerefer: A simple online baseline for referring video object segmentation. In *Proceedings of the IEEE/CVF International Conference on Computer Vision*, pages 2761–2770, 2023. 8
- [47] Jiannan Wu, Yi Jiang, Peize Sun, Zehuan Yuan, and Ping Luo. Language as queries for referring video object segmentation. In *Proceedings of the IEEE/CVF Conference on Computer Vision and Pattern Recognition*, pages 4974–4984, 2022. 1, 3, 8
- [48] Junfeng Wu, Yi Jiang, Wenqing Zhang, Xiang Bai, and Song Bai. Seqformer: a frustratingly simple model for video instance segmentation. *arXiv preprint arXiv:2112.08275*, 1(2):6, 2021. 1, 3
- [49] Zhao Yang, Jiaqi Wang, Yansong Tang, Kai Chen, Hengshuang Zhao, and Philip HS Torr. Lavt: Language-aware vision transformer for referring image segmentation. In *Proceedings of the IEEE/CVF Conference on Computer Vision and Pattern Recognition*, pages 18155–18165, 2022. 9
- [50] Zongxin Yang, Yunchao Wei, and Yi Yang. Associating objects with transformers for video object segmentation. *Advances in Neural Information Processing Systems*, 34:2491–2502, 2021. 1
- [51] Qinghao Ye, Haiyang Xu, Guohai Xu, Jiabo Ye, Ming Yan, Yiyang Zhou, Junyang Wang, Anwen Hu, Pengcheng Shi, Yaya Shi, et al. mplug-owl: Modularization empowers large language models with multimodality. *arXiv preprint arXiv:2304.14178*, 2023. 4
- [52] Hang Zhang, Xin Li, and Lidong Bing. Video-llama: An instruction-tuned audio-visual language model for video understanding. *arXiv preprint arXiv:2306.02858*, 2023. 4
- [53] Shilong Zhang, Peize Sun, Shoufa Chen, Min Xiao, Wenqi Shao, Wenwei Zhang, Kai Chen, and Ping Luo. Gpt4roi: Instruction tuning large language model on region-of-interest. *arXiv preprint arXiv:2307.03601*, 2023. 4
- [54] Tao Zhang, Xiangtai Li, Hao Fei, Haobo Yuan, Shengqiong Wu, Shunping Ji, Chen Change Loy, and Shuicheng Yan. Omg-llava: Bridging image-level, object-level, pixel-level reasoning and understanding. *arXiv preprint arXiv:2406.19389*, 2024. 4
- [55] Tao Zhang, Xingye Tian, Yu Wu, Shunping Ji, Xuebo Wang, Yuan Zhang, and Pengfei Wan. Dvis: Decoupled video instance segmentation framework. In *Proceedings of the IEEE/CVF International Conference on Computer Vision*, pages 1282–1291, 2023. 3
- [56] Tao Zhang, Xingye Tian, Yikang Zhou, Shunping Ji, Xuebo Wang, Xin Tao, Yuan Zhang, Pengfei Wan, Zhongyuan Wang, and Yu Wu. Dvis++: Improved decoupled framework for universal video segmentation. *arXiv preprint arXiv:2312.13305*, 2023. 3

- [57] Tao Zhang, Xingye Tian, Yikang Zhou, Yu Wu, Shunping Ji, Cilin Yan, Xuebo Wang, Xin Tao, Yuan Zhang, and Pengfei Wan. 1st place solution for the 5th lsvos challenge: Video instance segmentation. *arXiv preprint arXiv:2308.14392*, 2023. 3
- [58] Yikang Zhou, Tao Zhang, Shunping Ji, Shuicheng Yan, and Xiangtai Li. Dvis-daq: Improving video segmentation via dynamic anchor queries. *arXiv preprint arXiv:2404.00086*, 2024. 3
- [59] Deyao Zhu, Jun Chen, Xiaoqian Shen, Xiang Li, and Mohamed Elhoseiny. Minigpt-4: Enhancing vision-language understanding with advanced large language models. *arXiv preprint arXiv:2304.10592*, 2023. 4
- [60] Xueyan Zou, Zi-Yi Dou, Jianwei Yang, Zhe Gan, Linjie Li, Chunyuan Li, Xiyang Dai, Harkirat Behl, Jianfeng Wang, Lu Yuan, et al. Generalized decoding for pixel, image, and language. In *Proceedings of the IEEE/CVF Conference on Computer Vision and Pattern Recognition*, pages 15116–15127, 2023. 9
- [61] Xueyan Zou, Jianwei Yang, Hao Zhang, Feng Li, Linjie Li, Jianfeng Wang, Lijuan Wang, Jianfeng Gao, and Yong Jae Lee. Segment everything everywhere all at once. *Advances in Neural Information Processing Systems*, 36, 2024. 9

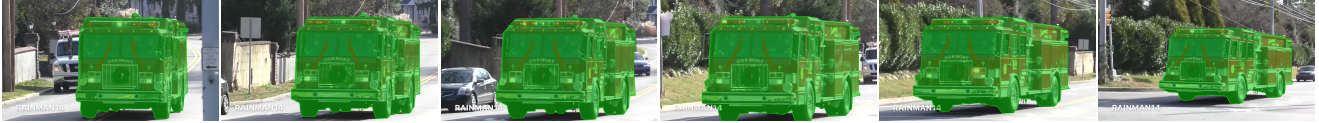
Appendix

A. Visualizations of Annotated Frames

Examples of annotated videos in ReVOS are shown in 6.



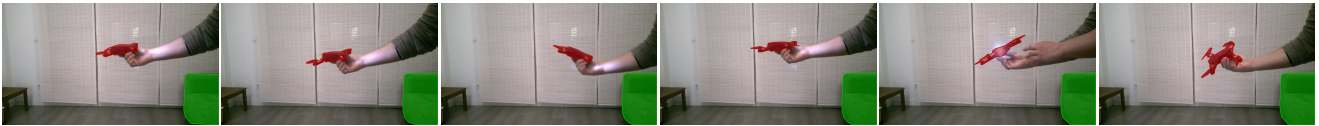
the walrus that loses the most gravitational potential energy.



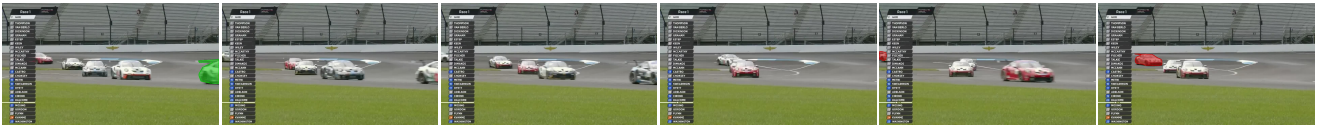
object that brushes off raindrops and dusty. What object in the video suggests there is a fire nearby?



labrador. Which dog's neck experiences more external force?



Which object has the capacity to fly? What the person might be resting on after the presentation?



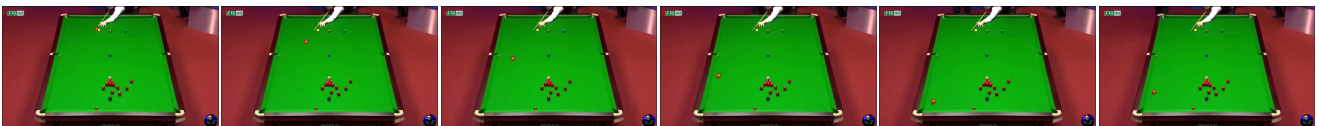
the last car to appear. the car most likely to win first place.



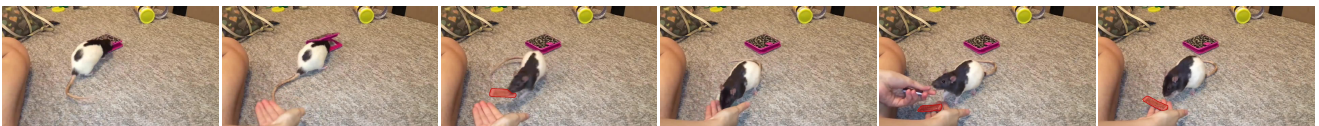
object ready to start hunting. Which animal in the video is most likely to die?



objects that simulate small animals.



the ball that should be hit first according to the rules. Which ball is the target of this shot?



What are the rats being trained to pick up in the video?

Figure 6. Sample videos in ReVOS.